River Flow 2020 – Uijttewaal et al (eds)

2D numerical modeling on meander chute cutoffs

Zhi Li & Marcelo H. García
Ven Te Chow Hydrosystems Laboratory, Department of Civil and Environmental Engineering, Grainger College of Engineering, University of Illinois at Urbana-Champaign, Urbana, USA

ABSTRACT: Reproduction of river meander cutoffs in laboratory has been found to be a challenging endeavor. In particular, stream bank failure is difficult to reproduce at small laboratory scales. Even though it may be much simpler to balance bank erosion and bank accretion with the help of numerical models, the difficulties to numerically model cutoffs remain. Existing numerical models for meander migration frequently tend to treat cutoffs as a fleet process. In this study, two distinctive but inter-related methods to model cutoffs are discussed. Both methods solve the 2D depth-averaged, unsteady Reynolds-averaged Navier–Stokes equations (URANS) coupled with k-ε model for turbulence closure. The Meyer-Peter Müller formula with the Exner equation are solved for bedload transport and bed morphology evolution. In the first method, the cutoff starts to develop through a process that periodically widens the chute cutoff channel. After each widening event, an originally non-erodible portion of floodplain collapses and becomes erodible. The coupling period of the widening process is subject to calibration. In the second method, the widening process is simulated with a hybrid deterministic-stochastic bank failure model. The widening process in this method is governed by the near bank sheer stress and the bank critical shear stress. The method assumes Gaussian distributions of both near bank shear stress and critical bank shear stress to evaluate the bank failure risk. Both methods are tested using a simplified bench scale chute cutoff, which is scaled down from a natural chute cutoff in the Wabash River, between Illinois and Indiana, USA.

1 INTRODUCTION

Cutoffs are captivating features of meandering rivers. After a chute cutoff event, the former secondary channel captures most of the flow and becomes the new main channel. The original main channel becomes a secondary one and eventually loses its depth, preventing navigation and other uses. This change in roles always brings people living by the river a dramatic alteration of their lives as well as a long-term impact.

To understand the cutoff dynamics, recent research efforts have focused on the phenomenological analysis of observations in nature (e.g. Zinger et al., 2011) and experiments in the laboratory (Van Dijk et al., 2012). On the other hand, not much research has been devoted to designing numerical models specifically for cutoffs. Over the years, many numerical modeling frameworks, methods and tools were proposed to simulate meander migration (e.g. Sun et al., 1996; Darby et al., 2002; Abad & Garcia, 2006; Motta et al., 2012). These numerical methods are mostly designed for long-term meander migration study; hence, their treatments of cutoffs are simplified to allow for long time-scale predictions.

In this study, we developed an integrated numerical model to simulate the chute channel evolution and oxbow lake formation. The model breaks some limitations that existing models set. It does not comprise the conventional bank erosion analysis including only elevation and cross-sectional directions, so that it can handle much more complex geometries, including asymmetric bifurcations and confluences in river bends. The model also considers the stochastic components during chute channel evolution. The model is tested through a set of numerical experiments in a simplified, bench-scale, chute cutoff.

2 METHODS

2.1 *Hydrodynamic model TELEMAC-2D and morphodynamic model SISYPHE*

The depth-averaged unsteady Reynolds Averaged Navier-Stokes equations (URANS) are solved using the finite element method. The standard κ-ε model is used for turbulence closure. The correction for curvature-induced secondary flow is included by solving an extra transport equation for ω.

The Meyer-Peter and Müller formula is applied for bedload transport. The bed slope effect, the secondary flow effect and the sediment slide effect due to angle of repose are considered in the model. The Exner equation is solved for bed evolution.

2.2 *First bank failure modeling method: Periodic chute channel widening*

Bank retreat is modeled as a periodic chute channel widening process. After each widening, an originally non-erodible portion of floodplain material collapses and becomes erodible riverbed material. This bank failure process is mass conservative.

2.3 *Second bank failure modeling method: Hybrid deterministic-stochastic method governed chute channel widening*

Adapted from the "risk of sediment erosion and suspension in turbulent flows" concept in Lopez & Garcia (2001), a similar way to evaluate the "risk of bank failure" is introduced:

The near-bank shear stress ($\bar{\tau}_f$) and the critical shear stress ($\bar{\tau}_c$) are randomized and assumed to have Gaussian distributions, whose PDFs and CDFs are ϕ_f, ϕ_c, $\boldsymbol{\phi}_f$ and $\boldsymbol{\phi}_c$, respectively. The bank failure risk R is evaluated through the probability of $\tau > \tau_c$, for any τ on the distribution ϕ_f, i.e.:

$$R = \int_{-\infty}^{+\infty} \boldsymbol{\phi}_c(\tau)\phi_f(\tau)d\tau = \boldsymbol{\phi}\left[4\left(\bar{\tau}_f - \bar{\tau}_c\right)/\sqrt{\bar{\tau}_f^2 + \bar{\tau}_c^2}\right] \quad (1)$$

where the factor 4 comes from the four-sigma rule.

The occurrence of bank failure is modeled as a Bernoulli process with p = R, which has two possible outcomes: success or failure. If the floodplain dry node passes the Bernoulli trial, it collapses and becomes a wet node in the channel. This bank failure process is mass conservative.

Finally, an integrated hydrodynamic (deterministic), bedload transport (deterministic) and bank failure (stochastic) numerical model is presented including some preliminary results.

2.4 *Numerical experiments setup*

To study the behavior of the proposed numerical model, we designed a group of numerical experiments. The geometry of the bench scale meandering river is based on the chute-cutoff flume in Ven Te Chow Hydrosystems Laboratory, UIUC. There are three meander bends in the experimental river following a sine-generated formula (see Figure 1a). The simulations presented herein were performed assuming a bank-full discharge, Q = 6 L/s. Key parameters are listed in Table 1.

The initial riverbed topography in the meandering channel is achieved through long time hydrodynamic and morphodynamic modeling. Once the rhythmic sequence of bars and pools is obtained, a 0.13m-wide and 0.03m-deep initial chute channel is created to prepare for the next chute cutoff numerical experiments (see Figure 1b).

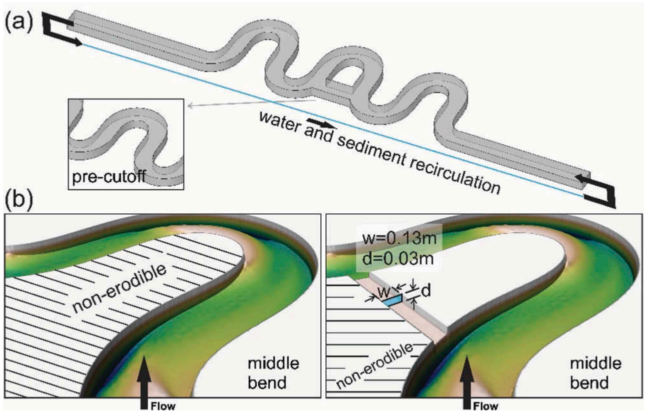

Figure 1. (a) The configuration of the virtual flume used in the numerical experiments. (b) Initial riverbed topography and the initial chute cutoff channel.

Table 1. Key parameters in the numerical experiments.

Physical Parameters		Numerical Parameters	
Width	0.52 m	Time step	0.005 s
Width-to-depth ratio	10	Mesh sizes	0.01-0.15 m
Slope	0.1%	Number of elements	270K
Froude number	0.3		
Reynolds number	11K		
Sediment particle Reynolds number	11.4 (fine sand)		
Manning's n in channel	0.02		
Manning's n on floodplain	0.1		

3 RESULTS

3.1 *First bank failure modeling method: Periodic chute channel widening*

In this method, the chute channel is widened periodically (every 12h in the present group of numerical experiments). The initial chute channel width is 25% of the main channel width. The width increment of each widening is same as the initial chute channel width. Thus, in total, there are 4 stages with increasing chute channel widths, 25%, 50%, 75% and 100% of the main channel width (see Figure 2-5).

Figure 2 shows the bed evolution in the first 12 hours after the creation of the initial chute channel. Figure 2a shows the riverbed degradation of chute channel. Figure 2b-d reveal the initiation of the sand bar at the left side of the entrance of the chute channel. This flow separation induced sand bar agrees with the findings in Dutta et al. (2017). Figure 3 shows the next 12-hour bed evolution after the first widening. In Figure 3a-c, the failed floodplain material is being dumped into the river channel. In Figure 2d, the floodplain material completely transformed to bed material, making a sand bar after the confluence point. At the same time, the bar at the left side of the entrance of the chute channel grows larger. Figure 4 shows the bed evolution after the second widening. The comparison between Figure 3a-c and 4a-c indicates the bank failure process is much faster after the second widening, implying the chute channel already captured the main flow. Figure 5 shows the bed evolution after the last widening. The chute channel width reaches the main channel width and it captures >90% flow at this phase.

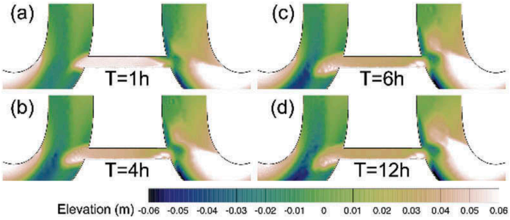

Figure 2. Bed evolution when chute channel width is 25% of the main channel width. Flow is from right to left.

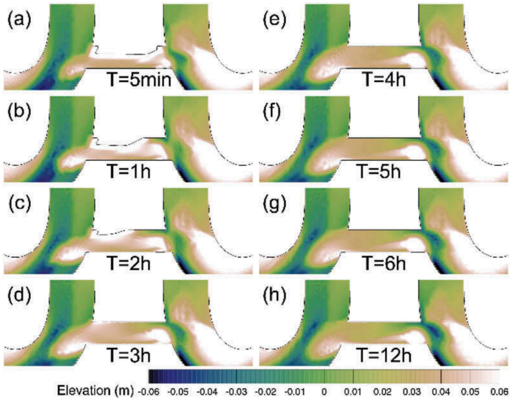

Figure 3. Bed evolution when chute channel width is 50% of the main channel width.

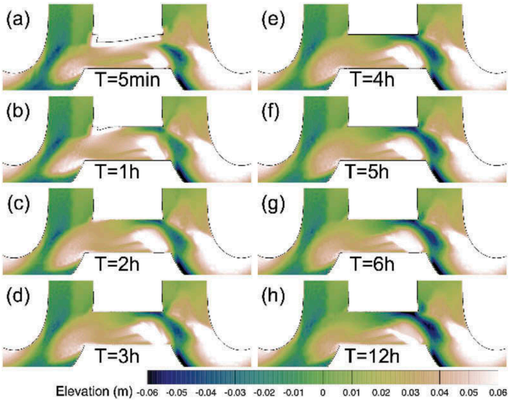

Figure 4. Bed evolution when chute channel width is 75% of the main channel width.

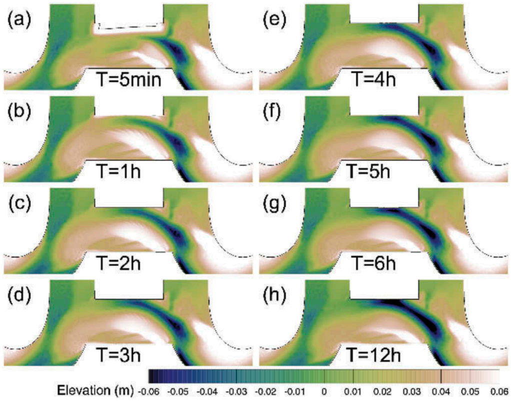

Figure 5. Bed evolution when chute channel width is 100% of the main channel width.

3.2 *Second bank failure modeling method: Hybrid deterministic-stochastic method governed chute channel widening*

In this method, as shown in Equation 1, the bank critical shear stress can control the riverbank erodibility. In the following two subsections, one realization of lower bank critical shear stress (higher bank erodibility) case and one realization of higher bank critical shear stress (lower bank erodibility) case are tested.

3.2.1 *Modeling soft bank with relatively high bank erodibility*

Since the geometry of the modeled channel is scaled down from the Mackey Bend, the modeling results show a great similarity compared to the satellite imagery (Figure 6). In both real-world cutoff and the modeled cutoff, 1) in the abandoned channel, a plug bar locates at the right side of the upstream limb; 2) in the chute channel, a sand bar locates at the left side near the entrance; 3) after the confluence point, and a sand bar locates at the left side of the channel.

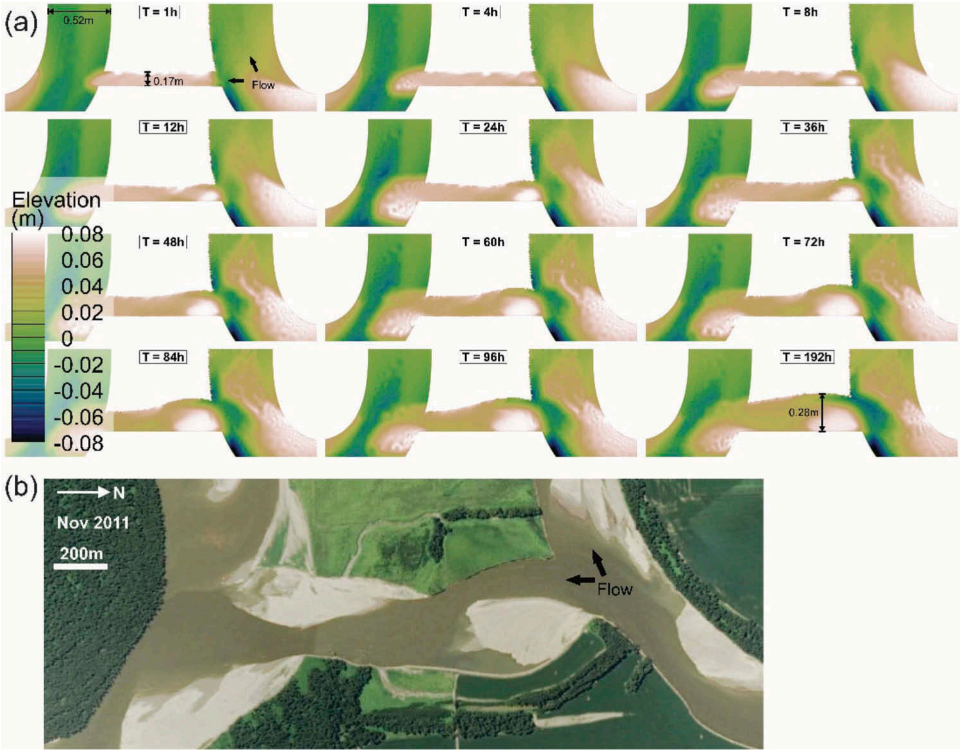

Figure 6. (a) The planform view of the bed evolution (relatively high bank erodibility case). (b) The chute cutoff generated complex sand bar depositions at the Mackey Bend, Wabash River, Illinois-Indiana, USA. The imagery from Google Earth is captured during low flow condition.

3.2.2 *Modeling stiff bank with relatively low bank erodibility*

Figure 7 suggests with lower bank erodibility, the widening process is much slower, and it takes much longer time for the chute channel to reach the main channel width. However, the location of the sand bar result from flow separation does not change.

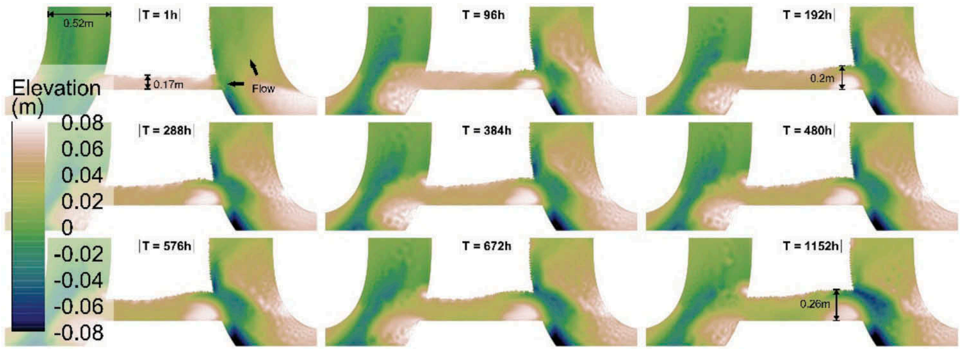

Figure 7. The planform view of the bed evolution (relatively low bank erodibility case). Note that the chute channel took about 6× more time to achieve the same width as in the higher bank erodibility case.

4 DISCUSSIONS AND CONCLUSIONS

This study provides two methods to numerically model chute cutoffs. The first method models bank retreat in chute channel is uniform in both time and space, while the second method is nonuniform and stochastic. By performing the lab-scale chute cutoff numerical experiments, both methods have successfully simulated the bed evolution from the initiation of the chute cutoff to the stage that it becomes the main channel. Both methods can handle complex geometries, predict chute cutoff channel migration and bed evolution. Moreover, both have acceptable computing efficiencies.

In particular, the second method provides a new look that cutoffs are modeled in a hybrid deterministic-stochastic framework. In theory, N times of simulations can yield N distinguished bank evolution trajectories. By doing ensemble averaging over multiple simulations could possibly produce a useful bank evolution pattern and statistics. This portion of the work remains to be done.

The model has the following highlighted features:

- Tightly coupling of hydrodynamics and morphodynamics and the ability to handle complex geometries.
- Dynamic assignment of bottom roughness in the whole floodplain-river system.
- Capability to model a full range of bank erodibility properties from rigid bank to extremely soft bank.
- Strict compliance of mass-conservation during the entire cutoff process.
- No constant width, constant slope, constant flow discharge or constant sediment load assumptions applied.
- Capture of pseudo-3D bank failure process.

ACKNOWLEDGEMENTS

The support of the Metropolitan Water Reclamation District of Greater Chicago (MWRDGC) is gratefully acknowledged. Support from the M.T. Geoffrey Yeh Chair in Civil Engineering is also acknowledged.

REFERENCES

Abad, J. D. & Garcia, M. H. 2006. RVR Meander: A toolbox for re-meandering of channelized streams. *Computers & Geosciences*, 32, 92–101.

Darby, S. E., Alabyan, A. M. & Van de Wiel, M. J. 2002. Numerical simulation of bank erosion and channel migration in meandering rivers. *Water Resources Research*, 38.

Dutta, S., Wang, D. C., Tassi, P. & Garcia, M. H. 2017. Three-dimensional numerical modeling of the Bulle effect: the nonlinear distribution of near-bed sediment at fluvial diversions. *Earth Surface Processes and Landforms*, 42, 2322–2337.

Lopez, F. & Garcia, M. H. 2001. Risk of sediment erosion and suspension in turbulent flows. *Journal of Hydraulic Engineering-Asce*, 127, 231–235.

Motta, D., Abad, J. D., Langendoen, E. J. & Garcia, M. H. 2012. A simplified 2D model for meander migration with physically-based bank evolution. *Geomorphology*, 163, 10–25.

Sun, T., Meakin, P., Jossang, T. & Schwarz, K. 1996. A simulation model for meandering rivers. *Water Resources Research*, 32, 2937–2954.

Van Dijk, W. M., Van de Lageweg, W. I. & Kleinhans, M. G. 2012. Experimental meandering river with chute cutoffs. *Journal of Geophysical Research-Earth Surface*, 117.

Zinger, J. A., Rhoads, B. L. & Best, J. L. 2011. Extreme sediment pulses generated by bend cutoffs along a large meandering river. *Nature Geoscience*, 4, 675–678.